

CHARACTERIZATION OF PHOTOCATHODE DAMAGE DURING HIGH CURRENT OPERATION OF THE CORNELL ERL PHOTOINJECTOR *

Jared Maxson[†], Luca Cultrera, Ivan Bazarov, Bruce Dunham, Sergey Belomestnykh, John Dobbins, Siddharth Karkare, Roger Kaplan, Vaclav Kostroun, Yulin Li, Xianghong Liu, Florian Löhl, Karl Smolenski, Zhi Zhao, David Rice, Peter Quigley, Maury Tigner, Vadim Veshcherevich, Kenneth Finkelstein, Darren Dale, Benjamin Pichler
CLASSE, Cornell University, Ithaca NY 14850, USA

Abstract

The Cornell ERL Photoinjector prototype has recently demonstrated successful operation at 20 mA for 8 hours using a bi-alkali photocathode grown on a Si substrate. The photocathode film was grown off center, and remained relatively undamaged; however, upon removal from the gun, the substrate at the gun electrostatic center displayed significant visible damage. Here we will describe not only the parameters of that particular high current run, but a suite of post-operation surface morphology and crystallographic measurements, including X-ray fluorescence, X-ray diffraction, and contact profilometry, performed about the damage site and photocathode film. The data indicate violent topological changes to the substrate surface, as well as significant induced crystallographic strain. Ion back-bombardment is proposed as a possible mechanism for damage, and a simple model for induced crystal strain is proposed (as opposed to ion induced sputtering), and is shown to have good qualitative agreement with the spatial distribution of damage.

INTRODUCTION

The high peak brightness beams required for next generation X-ray sources may be feasibly provided by photoelectron linacs. However, for high duty factor, high average brightness operation, the preservation of the photocathode quantum efficiency (QE), remains a significant operational challenge. In this report, we describe the operation of the Cornell ERL photoinjector prototype at a CW current of 20mA for 8 hours [1], using a K_2CsSb photocathode. A schematic of the Cornell ERL injector is shown in Fig. 1. Since that particular run, the Cornell photoinjector has operated up to 50mA, but for much shorter time periods using a GaAs photocathode [2]. In this particular run, we determine K_2CsSb to be suitably rugged for time scales of operation at the high current required for a user facility.

The preservation of the photocathode throughout the run is in large part due to the growth of the film away from the electrostatic center, where a large damage site is visible by eye. The current as a function of time in the run is shown in Fig. 2. Beam current was held constant with a fast laser feedback, interrupted only by vacuum bursts

intermittently. No significant decrease in the quantum efficiency was noted, via the lack of increase in the overall laser power. An image of the photocathode surface and the QE map are shown in Fig. 3.

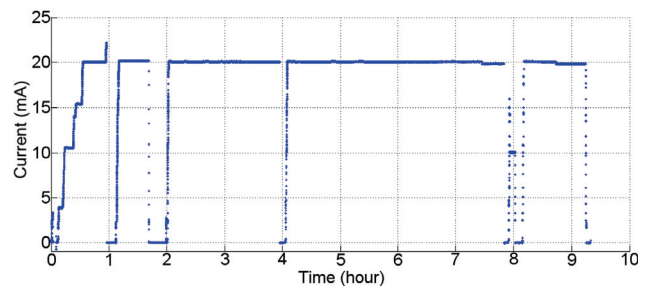


Figure 2: Current as a function of time for the run in question. Dips in current correspond to vacuum trips.

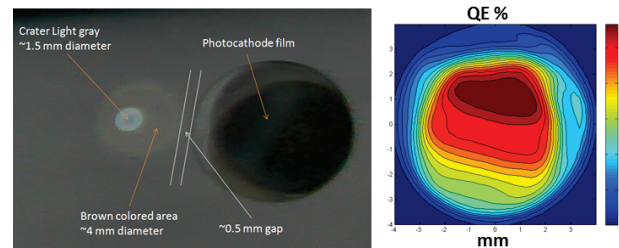


Figure 3: Left: Photograph of the photocathode after use. Heavy damage accumulates at the gun electrostatic center. Right: QE map of the film after the run. No overall QE decrease was detected throughout the run.

SURFACE ANALYSIS

The recipe for the photocathode deposition has been described elsewhere [3]. We believe that the non-uniformity of the QE distribution to be the spatial mismatch of the elements during deposition. This was measured by X-ray Fluorescence (XRF) at the Cornell High Energy Synchrotron Source (CHESS). XRF measurements were calibrated to give the actual areal density via the use of single element deposition measured with both Rutherford Backscattering Spectroscopy and XRF. These calibrated elemental maps are shown in Fig. 4.

* This work supported by the NSF under Grant No. DMR-0807731

[†] jmm586@cornell.edu

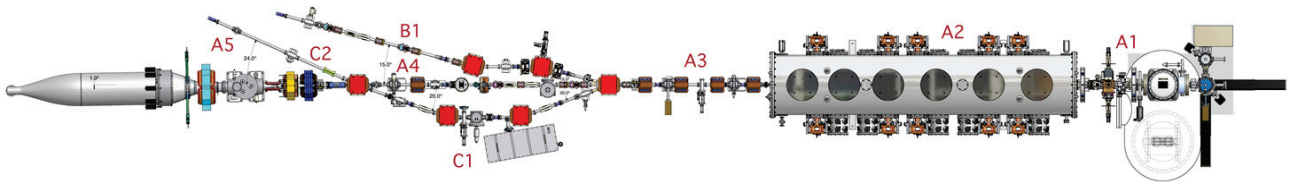


Figure 1: A schematic of the Cornell ERL photoinjector. Beam travels from right to left.

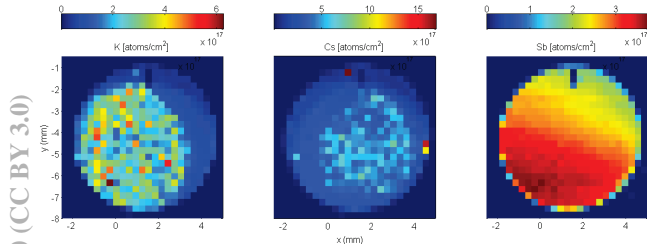


Figure 4: Element areal density measured with XRF at CHESS.

With the knowledge that ions from the residual gas along the beamline can travel backwards and strike the photocathode surface, our initial impression of the central damage site was that of a crater. However, surface contact profilometry reveals that it is not a crater, but rather a damage mound, as shown in Fig. 5. This, coupled with simulations of ion penetration and sputtering using TRIM [7], suggests that the mechanism of damage is not sputtering of material from the substrate surface. Furthermore, the density of amorphous Si is 30% larger than crystalline Si, and using ion tracking data to calculate ion penetration depth [1], we conclude that the mound formation is not caused by the amorphization of the substrate. Large doses of ions via implantation have been known to cause the formation of micro-pores beneath the surface [4]; whether this is the mechanism of the mound formation remains an open question as SEM analysis of the cleaved sample was inconclusive [1].

Prior to cleaving, X-ray diffraction was performed in the Bragg geometry to analyze the distribution of crystal strain (seen as a displacement of the atomic plane d -spacing). The Bragg angle was varied, and the intensity of the diffracted X-rays was imaged with an X-ray CCD. In doing so, we found that the strain distribution was highly radial, owing to the radial symmetry of the beam, and thus the symmetry of the backwards traveling ion beam. Thus, the images were sliced along a diameter of the substrate, and the intensity of diffracted x-rays as a function of Bragg angle and position along the diameter is plotted in Fig. 6. The intense band near $\theta = 17.5^\circ$ corresponds to the bulk Si diffraction.

Here, we see that close to the electrostatic center, the crystal strain ($\propto \theta$) increases, but at the center, the high strain diffraction ceases, and only diffraction from the bulk remains. We believe that this drop-off corresponds to the full amorphization of the substrate surface, which cannot

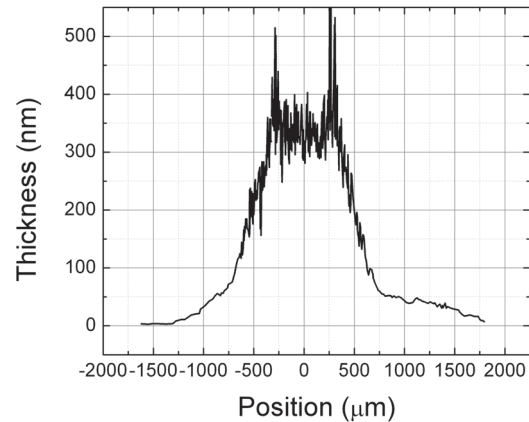


Figure 5: Contact profilometry of the central damage site, indicating the presence of a mound.

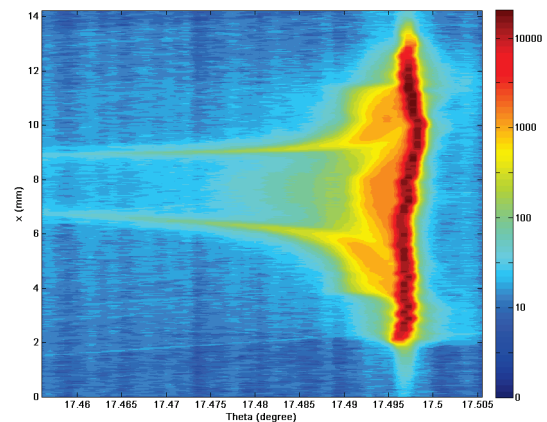


Figure 6: Intensity of diffracted x-rays vs. Bragg angle and radial position along the central damage site.

not produce strong Bragg reflection.

MODELING THE STRAIN DISTRIBUTION

Owing to the highly radial nature of the damage to the substrate, it is likely that the cause of the damage is the bombardment of the photocathode by backwards traveling ions from the residual gas. We assume that ions are

Table 1: Top: Partial pressures of the dominant residual gas species, as measured by RGA within the DC gun chamber. Bottom: Ion beam composition, calculated from partial pressure and ionization cross section.

| Species | Partial Pressure (torr) |
|------------------|-------------------------|
| H ₂ | 1×10^{-11} |
| H ₂ O | 1×10^{-12} |
| CO | 5×10^{-13} |
| CO ₂ | 1×10^{-13} |

| Species | Percent composition |
|-------------------------------|---------------------|
| H ₂ ⁺ | 75% |
| H ₂ O ⁺ | 5% |
| CO ⁺ | 15% |
| CO ₂ ⁺ | 5% |

predominately produced in the section prior to the SRF booster, owing to the strong cryopumping of the SRF linac, as well as the inherent RF rejection of the ion beam. To calculate the overall ion dose, we use the ionization cross section, beam current, and baseline partial pressure in the beam pipe. Using the parameters in Table 1, we calculate a total ion production rate of 1.85×10^9 ions/Coulomb, or 1.1×10^{12} ions over the course of the run. For simplicity, we assume that all compound ions are fully cracked at the photocathode surface, yielding single element ions. This enables the use of the transport of ions in material (TRIM) [7] software package. TRIM calculations reveal that at 250 kV hydrogen sputters negligibly; carbon and oxygen are between 10 and 20 percent. Neither of these is large enough to produce damage features on the scale noted above, and is ruled out as the dominant damage mechanism.

To model the spatial distribution of the ions, we use the beam density profile at the exit of the gun anode, calculated with ASTRA [6]. Following [5], we find that we can calculate the strain induced simply by knowledge of the ion dose and energy. A salient feature of the strain (parameterized as the percent of RBS dechanneling) vs. dose relationship is its “super-linearity”—the sharp rise of of the strain at a particular ion dose (for our case, 4×10^{14} ions/cm²). Beyond this dose, full amorphization (full RBS dechanneling) can be achieved in our system. We find that we need only supply an overall pressure 10× greater than the baseline pressure to achieve an amorphous region as large as seen in Fig. 6. We believe this to be a reasonable scaling of baseline pressure to account for the violent increase in pressure during the vacuum bursts which tripped the beam. The final RBS dechanneling/strain distribution is shown in Fig. 7, where a fully amorphous region is realized.

CONCLUSIONS

In this paper, we present the successful operation of the Cornell ERL photoinjector at a current of 20 mA CW for 8 hours with a K₂CsSb photocathode. While the current at the time was limited by the corresponding vacuum in-

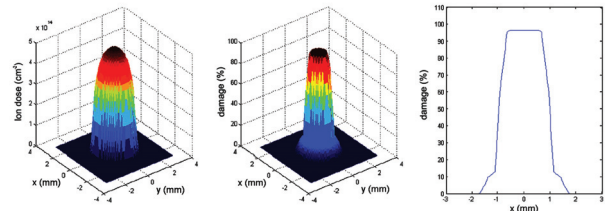


Figure 7: Left: The calculated total ion dose based on the simulated beam profile at the gun anode, using 10 times the baseline pressure. Middle and Right: Damage (or percent RBS dechanneling), calculated via the strain vs. ion dose in [5].

crease, the length of the run was not technologically limited. Over the course of the run, there was no apparent degradation of the photocathode QE, likely owing to the off-center deposition of the photocathode film. At the center of the substrate, a large damage mound was formed, the exact mechanism for which remains unresolved. Large crystal strain was noted with x-ray diffraction, and is argued to be due to ion back-bombardment. A simple model is proposed for the generation of the strain distribution, which agrees qualitatively with the measured distribution.

ACKNOWLEDGEMENTS

The ERL photoinjector program at Cornell University is supported by the NSF, under Award No. DMR-0807731. This work is based upon research conducted at the Cornell High Energy Synchrotron Source (CHESS) which is supported by the National Science Foundation and the National Institutes of Health/ National Institute of General Medical Sciences under NSF Award No. DMR-0936384. One of us (J. M.) is supported by the NSF Graduate Research Fellowship Program under Grant No. DGE-0707428, and one of us (L. C.) is supported by DOE No. DE-SC0003965.

REFERENCES

- [1] L. Cultrera et al., Phys. Rev. ST Accel. Beams 14, 120101 (2011).
- [2] B. Dunham et al., “Cornell ERL Photoinjector Progress,” MOOAA01, these proceedings.
- [3] L. Cultrera et al., “Growth and Characterization of Bialkali Photocathodes for Cornell ERL Injector,” PAC2011, New York, NY, March 2011, WEP244, p. 1944, <http://www.JACoW.org>
- [4] A. G. Perez-Bergquist, et. al., Nucl. Instrum. Methods Phys. Res., Sect. B 269, 561 (2011).
- [5] G. Bai and M. Nicolet, J. Appl. Phys. 71, 670 (1992).
- [6] K. Flottman, Astra: A space charge tracking algorithm, DESY (2000).
- [7] J. F. Ziegler, Nucl. Instrum. Methods Phys. Res., Sect. B 219, 1027 (2004).